JOURNAL OF GUIDANCE, CONTROL, AND DYNAMICS
Vol. 30, No. 4, July–August 2007

Engineering Notes

ENGINEERING NOTES are short manuscripts describing new developments or important results of a preliminary nature. These Notes should not exceed 2500 words (where a figure or table counts as 200 words). Following informal review by the Editors, they may be published within a few months of the date of receipt. Style requirements are the same as for regular contributions (see inside back cover).

Model Updating with Closed-Loop Strain Mode Shapes

Jaehoon Ha,* Youngjin Park,† and Younsik Park†
Korea Advanced Institute of Science and Technology, Daejeon 305-701, Republic of Korea

DOI: 10.2514/1.29491

I. Introduction

MODEL updating is a method of correcting analytical models, such as the finite element model, by improving the correlation between the measured data and the analytical model. The correlation can be determined by a penalty function that involves modal data such as natural frequencies and mode shapes [1,2]. However, a modal sensitivity matrix that is ill conditioned due to a lack of modal data can incur inaccurate model updating. For more efficient model updating, we need to increase the amount of modal data. Recently, some researchers have used closed-loop schemes to capture additional modal data [3,4]. Strain mode shapes have also been used instead of displacement mode shapes because of their perceived advantages [5,6]. For example, the difference in the strain mode shapes of an intact case and a damaged case is greater than the corresponding difference in the displacement mode shapes. This phenomenon explains why strain mode shapes are generally considered more sensitive than displacement mode shapes with respect to the local change of a structure. However, this property is valid when the local change of a structure can change the displacement mode shapes because strain mode shapes are spatial derivatives of displacement mode shapes.

If we simultaneously use strain mode shapes and the closed-loop scheme, we can enhance the performance of model updating. We, therefore, propose a novel method of combining strain mode shapes and the closed-loop scheme for effective model updating. In addition, to demonstrate the feasibility of the proposed method, we provide a numerical simulation of model updating based on the closed-loop strain mode shapes.

II. Model Updating with Modal Data

A. Combined Modal Sensitivity Matrix

Our method of using modal data for model updating relies on the following penalty function, which uses a truncated Taylor series expansion of the modal data with respect to the parameters:

$$\delta \mathbf{z} = \mathbf{S}_j \delta \boldsymbol{\theta} \tag{1}$$

where $\delta\boldsymbol{\theta} = \boldsymbol{\theta} - \boldsymbol{\theta}_j$ is the perturbation in the parameters, $\delta\mathbf{z} = \mathbf{z}_m - \mathbf{z}_j$ is the error in the measured modal data, $\mathbf{S}_j$ is the modal sensitivity matrix, and j is the number of iterations. This set of equations is usually ill conditioned because of insufficient modal data. If the amount of modal data is increased, we can make the modal sensitivity matrix well conditioned. To this end, we suggest to use a feedback control idea, such as the mode decoupling controller [4]. If the additional modal data are measured, the combined sensitivity matrix can be obtained as

$$\mathbf{T} = \begin{bmatrix} \mathbf{S}^o & \mathbf{S}^{c_1} & \mathbf{S}^{c_2} & \cdots & \mathbf{S}^{c_i} \end{bmatrix}^T \tag{2}$$

where the superscript o represents an open loop and the superscript c_i represents a closed loop.

B. Strain-Based Equation of Motions and the Associated Modal Sensitivity Matrix

Strain quantities are generally less frequently used for acquiring modal data than accelerations or displacements. If we collect strains as the output quantities for modal testing, we can measure the associated modal data, such as the natural frequencies and the strain mode shapes. In this case, if the equation of motions for an analytical model can be represented by strain quantities, we can conveniently compare the measured data and the analytical model. Furthermore, a strain-based equation of motion is helpful when we analytically derive a strain-based modal sensitivity matrix for model updating.

Because of the above-mentioned reasons, we elucidate the strain-based equation of motions as briefly as possible [7]. To begin with, we applied a substructural representation to the system energy as follows:

$$\boldsymbol{\Pi}(\mathbf{u}, \boldsymbol{\lambda}, \mathbf{u}_g) = \mathbf{u}^T \left(\tfrac{1}{2}\mathbf{K}\mathbf{u} - \mathbf{f} + \mathbf{M}\ddot{\mathbf{u}} + \mathbf{D}\dot{\mathbf{u}} \right) + \boldsymbol{\lambda}^T \mathbf{B}_\lambda^T (\mathbf{u} - \mathbf{L}\mathbf{u}_g) \tag{3}$$

where $\mathbf{M}$, $\mathbf{D}$, and $\mathbf{K}$ are the substructural mass, the damping, and the stiffness matrices, respectively; $\boldsymbol{\lambda}$ represents the localized Lagrangian multipliers; $\mathbf{u}$ and $\mathbf{u}_g$ are the substructural and assembled displacements; $\mathbf{L}$ is the disassembly Boolean matrix that relates the assembled and substructural displacements; and $\mathbf{B}_\lambda$ is a Boolean operator that extracts the partition boundary nodes of all the partitioned substructures. To represent the equation of motions based on the strain quantities, we need to use the following strain-to-displacement relation:

$$\mathbf{u} = \boldsymbol{\Phi}\mathbf{q} = \boldsymbol{\Phi} \begin{bmatrix} \mathbf{s}^T & \boldsymbol{\alpha}^T \end{bmatrix}^T \tag{4}$$

where $\boldsymbol{\Phi}$ is the strain-to-displacement relation matrix, $\mathbf{s}$ is the strain variable, and $\boldsymbol{\alpha}$ is the rigid-mode amplitude. If $\mathbf{u}$ is replaced with $\boldsymbol{\Phi}\mathbf{q}$ in Eq. (3), we can restate the system energy as

$$\boldsymbol{\Pi}(\mathbf{q}, \boldsymbol{\lambda}, \mathbf{u}_g) = (\boldsymbol{\Phi}\mathbf{q})^T \left(\tfrac{1}{2}\mathbf{K}\boldsymbol{\Phi}\mathbf{q} - \mathbf{f} + \mathbf{M}\boldsymbol{\Phi}\ddot{\mathbf{q}} + \mathbf{D}\boldsymbol{\Phi}\dot{\mathbf{q}} \right) + \boldsymbol{\lambda}^T \mathbf{B}_\lambda^T (\boldsymbol{\Phi}\mathbf{q} - \mathbf{L}\mathbf{u}_g) \tag{5}$$

Thus, the stationary value of $\delta\boldsymbol{\Pi}$ produces the following matrix equation set:

Received 27 December 2006; revision received 16 March 2007; accepted for publication 20 March 2007.

*Graduate Student, Department of Mechanical Engineering, Science Town.
†Professor, Department of Mechanical Engineering, Science Town.

$$\begin{bmatrix} \mathbf{M}_\phi(d^2/dt^2)+\mathbf{D}_\phi(d/dt)+\mathbf{K}_\phi & \mathbf{\Phi}^T\mathbf{B}_\lambda & \mathbf{0} \\ \mathbf{B}_\lambda^T\mathbf{\Phi} & \mathbf{0} & -\mathbf{L}_b \\ \mathbf{0} & -\mathbf{L}_b^T & \mathbf{0} \end{bmatrix} \begin{bmatrix} \mathbf{q} \\ \boldsymbol{\lambda} \\ \mathbf{u}_g \end{bmatrix} = \begin{bmatrix} \mathbf{\Phi}^T\mathbf{f} \\ \mathbf{0} \\ \mathbf{0} \end{bmatrix} \tag{6}$$

where $\mathbf{M}_\phi = \mathbf{\Phi}^T\mathbf{M}\mathbf{\Phi}$, $\mathbf{D}_\phi = \mathbf{\Phi}^T\mathbf{D}\mathbf{\Phi}$, $\mathbf{K}_\phi = \mathbf{\Phi}^T\mathbf{K}\mathbf{\Phi}$, and $\mathbf{L}_b = \mathbf{B}_\lambda^T\mathbf{L}$. We can then rearrange the first row in Eq. (6) as

$$\mathbf{M}_\phi\ddot{\mathbf{q}} = \mathbf{b} - \mathbf{\Phi}_b\boldsymbol{\lambda}, \qquad \mathbf{\Phi}_b = \mathbf{\Phi}^T\mathbf{B}_\lambda, \qquad \mathbf{b} = \mathbf{\Phi}^T\mathbf{f} - \mathbf{D}_\phi\dot{\mathbf{q}} - \mathbf{K}_\phi\mathbf{q} \tag{7}$$

After two time differentiations, we can state the second row of Eq. (6) as

$$\mathbf{\Phi}_b^T\ddot{\mathbf{q}} - \mathbf{L}_b\ddot{\mathbf{u}}_g = \mathbf{0} \tag{8}$$

which, if Eq. (7) is used, becomes

$$\mathbf{\Phi}_b^T\mathbf{M}_\phi^{-1}(\mathbf{b} - \mathbf{\Phi}_b\boldsymbol{\lambda}) - \mathbf{L}_b\ddot{\mathbf{u}}_g = \mathbf{0} \tag{9}$$

We can therefore yield $\boldsymbol{\lambda}$ as follows:

$$\boldsymbol{\lambda} = \mathbf{M}_b\left(\mathbf{\Phi}_b^T\mathbf{M}_\phi^{-1}\mathbf{b} - \mathbf{L}_b\ddot{\mathbf{u}}_g\right), \qquad \mathbf{M}_b = \left(\mathbf{\Phi}_b^T\mathbf{M}_\phi^{-1}\mathbf{\Phi}_b\right)^{-1} \tag{10}$$

Next, by inserting Eq. (10) into the last row of Eq. (6), we obtain the following:

$$\ddot{\mathbf{u}}_g = \mathbf{M}_L^{-1}\mathbf{L}_b^T\mathbf{M}_b\mathbf{\Phi}_b^T\mathbf{M}_\phi^{-1}\mathbf{b}, \qquad \mathbf{M}_L = \mathbf{L}_b^T\mathbf{M}_b\mathbf{L}_b \tag{11}$$

From Eqs. (10) and (11), $\boldsymbol{\lambda}$ is derived as

$$\boldsymbol{\lambda} = \mathbf{P}_b\mathbf{\Phi}_b^T\mathbf{M}_\phi^{-1}\mathbf{b}, \qquad \mathbf{P}_b = \mathbf{M}_b - \mathbf{M}_b\mathbf{L}_b\mathbf{M}_L^{-1}\mathbf{L}_b^T\mathbf{M}_b \tag{12}$$

By eliminating $\boldsymbol{\lambda}$ from Eqs. (6) and (12), we can then obtain the following equation:

$$\mathbf{M}_\phi\ddot{\mathbf{q}} = \mathbf{b} - \mathbf{\Phi}_b\boldsymbol{\lambda} = \mathbf{b} - \mathbf{\Phi}_b\mathbf{P}_b\mathbf{\Phi}_b^T\mathbf{M}_\phi^{-1}\mathbf{b} = \mathbf{P}_\phi\mathbf{b}, \qquad \mathbf{P}_\phi = \left(\mathbf{I} - \mathbf{\Phi}_b\mathbf{P}_b\mathbf{\Phi}_b^T\mathbf{M}_\phi^{-1}\right) \tag{13}$$

which can be rearranged as follows in a standard second-order form:

$$\mathbf{M}_\phi\ddot{\mathbf{q}} + \mathbf{P}_\phi\mathbf{D}_\phi\dot{\mathbf{q}} + \mathbf{P}_\phi\mathbf{K}_\phi\mathbf{q} = \mathbf{P}_\phi\mathbf{f}_\phi, \qquad \mathbf{f}_\phi = \mathbf{\Phi}^T\mathbf{f} \tag{14}$$

To derive the strain modal sensitivity matrix, we use the modal sensitivity matrix which contains the first derivative of the strain mode shapes with respect to the updating parameters. The first derivative of the strain mode shapes can then be derived from Eq. (14) for a nonself-adjoint case as follows:

$$\frac{\partial\boldsymbol{\psi}_{R,j}}{\partial\theta} = -\frac{1}{2}\left(\boldsymbol{\psi}_{L,j}^T\frac{\partial\mathbf{M}_\phi}{\partial\theta}\boldsymbol{\psi}_{R,j}\right)\boldsymbol{\psi}_{R,j} + \sum_{\substack{k=1\\k\neq j}}^{N}\frac{1}{\lambda_j-\lambda_k}\left(\boldsymbol{\psi}_{L,k}^T\left[\frac{\partial\mathbf{K}_\phi}{\partial\theta} - \lambda_j\frac{\partial\mathbf{M}_\phi}{\partial\theta}\right]\boldsymbol{\psi}_{R,j}\right)\boldsymbol{\psi}_{R,k} \tag{15}$$

where $\boldsymbol{\psi}_{R,j}$ and $\boldsymbol{\psi}_{L,j}$ are the right and left strain mode shapes at the jth mode, respectively, λ_j is the eigenvalue (the square of natural frequency) at the jth mode, and θ is an updating parameter. Equation (15) is a modified version of the first derivative of the displacement mode shapes which was proposed in [8]. By using Eq. (15), we can then build the combined modal sensitivity matrix for model updating.

III. Closed-Loop Systems for Model Updating

The strain-based equation of motions can be rewritten as follows to include a matrix output equation:

$$\mathbf{M}_\phi\ddot{\mathbf{q}} + \mathbf{P}_\phi\mathbf{D}_\phi\dot{\mathbf{q}} + \mathbf{P}_\phi\mathbf{K}_\phi\mathbf{q} = \mathbf{P}_\phi\mathbf{\Phi}^T\mathbf{f} = \mathbf{P}_\phi\mathbf{\Phi}^T\mathbf{b}_2 r, \qquad \mathbf{y} = \mathbf{C}_{oq}\mathbf{q} \tag{16}$$

where $\mathbf{b}_2$ is the substructural input influence matrix, r is the exciter reference signal, $\mathbf{y}$ is the output vector, and $\mathbf{C}_{oq}$ is the output influence matrix. In addition, for simplicity, we assumed a proportional damping property. If we build the closed-loop systems via strain output feedback, the closed-loop equation of motions is derived as follows:

$$\mathbf{M}_\phi\ddot{\mathbf{q}} + \mathbf{P}_\phi\mathbf{D}_\phi\dot{\mathbf{q}} + \mathbf{P}_\phi\mathbf{K}_\phi\mathbf{q} = \mathbf{P}_\phi\mathbf{\Phi}^T\mathbf{b}_2(r - \mathbf{G}\mathbf{y}) = \mathbf{P}_\phi\mathbf{\Phi}^T\mathbf{b}_2(r - \mathbf{G}\mathbf{C}_{oq}\mathbf{q}) \tag{17}$$

The dynamic property of the closed-loop system depends on the gain vector $\mathbf{G}$ as in the following equation:

$$\mathbf{M}_\phi\ddot{\mathbf{q}} + \mathbf{P}_\phi\mathbf{D}_\phi\dot{\mathbf{q}} + \mathbf{P}_\phi\left(\mathbf{K}_\phi + \mathbf{\Phi}^T\mathbf{b}_2\mathbf{G}\mathbf{C}_{oq}\right)\mathbf{q} = \mathbf{P}_\phi\mathbf{\Phi}^T\mathbf{b}_2 r \tag{18}$$

Our calculation of the gain vector $\mathbf{G}$ follows the rule of the mode decoupling controller [4]. This controller can shift the target mode, thereby, leaving the nontarget mode unchanged and breaking the coupling of the modes. The gain vector $\mathbf{G}$ can be worked out through the open-loop strain mode shapes as follows:

$$\mathbf{G}^T = \text{Null}\left(\left[\,\hat{\boldsymbol{\psi}}_1 \quad \cdots \quad \hat{\boldsymbol{\psi}}_{t-1} \quad \hat{\boldsymbol{\psi}}_{t+1} \quad \cdots \quad \hat{\boldsymbol{\psi}}_l\,\right]^T\right) \tag{19}$$

where the open-loop strain mode shapes $\hat{\boldsymbol{\psi}} = \hat{\boldsymbol{\psi}}_R = \hat{\boldsymbol{\psi}}_L$ (which are due to the self-adjoint property) are determined from measurements, t is used to designate the target mode, and l is the number of modes. The strain mode shapes become real values because of the assumption of the proportional damping property. Any mode can be fixed if the number of sensors is equal to the number of modes. The gain vector for the mode decoupling controller can also be explained from a modal sensor point of view [9]. We can determine the gains and locations of the sensors to sense a target mode or a set of targeted modes; this kind of sensor is called a modal sensor. The output equation can then be expressed in modal coordinates as follows:

$$\mathbf{y} = \mathbf{C}_{oq}\mathbf{q} = \mathbf{C}_{oq}\boldsymbol{\psi}\mathbf{q}_m = \mathbf{C}_{mq}\mathbf{q}_m, \qquad \mathbf{C}_{oq}\boldsymbol{\psi} = \mathbf{C}_{mq} \tag{20}$$

If we say that $\mathbf{C}_{mq}(i) = 0$ if $i \neq t$, and $\mathbf{C}_{mq}(i) = 1$ if $i = t$, where $\mathbf{C}_{mq}$ is the $1 \times l$ modal output vector, we can obtain the influence matrix, $\mathbf{C}_{oq}$, as follows:

$$\mathbf{C}_{oq} = \mathbf{C}_{mq}\boldsymbol{\psi}^+ \tag{21}$$

Consequently, the unit-normalized $\mathbf{C}_{oq}$ from Eq. (21) and the gain vector $\mathbf{G}$ from Eq. (19) are the same. Therefore, the physical meaning of the gain vector for the mode decoupling controller can be interpreted as that of a modal sensor. Strictly speaking, the modal output feedback is incorporated into the mode decoupling controller.

If the strain mode shapes are mass normalized, we can rewrite Eq. (18) in modal coordinates as follows:

$$\mathbf{I}\,\ddot{\mathbf{q}}_m + 2\mathbf{Z}\mathbf{\Lambda}\,\dot{\mathbf{q}}_m + (\mathbf{\Lambda}^2 + \mathbf{b}_m\mathbf{g}_m)\mathbf{q}_m = \mathbf{b}_m r \qquad \text{where } \mathbf{b}_m = \boldsymbol{\psi}^T\mathbf{\Phi}^T\mathbf{b}_2, \quad \mathbf{g}_m = \mathbf{G}\mathbf{C}_{oq}\boldsymbol{\psi} \tag{22}$$

where $\mathbf{\Lambda}$ is a diagonal matrix of natural frequencies, $\mathbf{Z}$ is a modal damping matrix, and $\mathbf{b}_m$ is a modal input matrix. Thus, the closed-loop modal data can be expressed as follows:

Table 1 Beam thickness of each element as an updating parameter (unit: mm)

Element no.	2	3	4	5	6	7	8	9
Initial	5.00	5.00	5.00	5.00	5.00	5.00	5.00	5.00
Actual	4.80	4.70	4.40	4.20	3.70	4.00	3.80	4.30

Table 2 Results of updated parameters (unit: mm)

Element no.	2	3	4	5	6	7	8	9	Error norm
Actual	4.80	4.70	4.40	4.20	3.70	4.00	3.80	4.30	——
Case 2	6.50	4.11	5.17	3.89	3.87	4.05	3.80	4.52	2.00
Case 3	4.71	4.59	4.46	4.26	3.80	4.16	3.94	4.41	0.31
Case 4	4.78	4.74	4.42	4.17	3.76	3.97	3.89	4.33	0.13

$$\ddot{q}_{m,t} + 2\zeta_t\omega_t\dot{q}_{m,t} + (\omega_t^2 + b_{m,t}g_{m,t})q_{m,t} = b_{m,t}r$$
$$\ddot{q}_{m,k} + 2\zeta_k\omega_k\dot{q}_{m,k} + \omega_k^2 q_{m,k} = b_{m,k}(r - g_{m,t}q_{m,t}), \quad \text{where } k \neq t$$
$$\therefore\ {}_c\omega_t = \sqrt{\omega_t^2 + b_{m,t}g_{m,t}}, \qquad {}_c\zeta_t = \omega_t\zeta_t/\sqrt{\omega_t^2 + b_{m,t}g_{m,t}} \tag{23}$$

IV. Numerical Simulation: Beam Thickness Estimation

For comparison, we conducted a numerical simulation of model updating via accelerometers and strain gages. We assumed the standard deviation of the measurement noises in the mode shapes to be 5% of the true values, and we used a cantilever beam with a fixed-free boundary condition for the simulation. Next, we built a finite element model with 10 beam elements and the model has the following dimensions: the material density is 7.8×10^3 kg/m^3, the total length is 0.5 m, the nominal mean value of thickness is 4.4 mm, the width is 20 mm, and the Young's modulus is 2.1×10^{11} N/m. The displacement and strain mode shapes can be obtained in an open-loop system and in a closed-loop system. In the open-loop system, we considered the first and second mode shapes, which can usually be measured more accurately than higher modes. Subsequently, we used only the first mode shape in closed-loop system 1 and, similarly, we used only the second mode shape in closed-loop system 2. The first mode is the target mode in closed-loop system 1 and the second mode is the target mode in closed-loop system 2. Consequently, we used four mode shapes for the model updating and we selected the beam thickness of each element as an updating parameter. Table 1 shows the initial and actual beam thickness.

Figure 1 shows the excitation and measurement points for the accelerometers and strain gages. Note that each bending strain is evaluated through two axial strains and at the Barlow points [10]. After constructing the combined sensitivity matrix with the four displacement mode shapes and the four strain mode shapes with measurement errors, we used Eq. (1) for the model updating until the updating parameters converged. The results of the model updating are divided into four cases: 1) the displacement mode shapes without closed-loop modes, 2) the displacement mode shapes with closed-loop modes, 3) the strain mode shapes without closed-loop modes, and 4) the strain mode shapes with closed-loop modes. Table 2 shows the updated thickness according to each case.

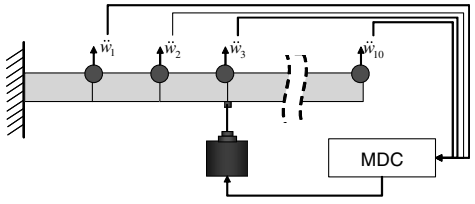

a) Acceleration output feedback

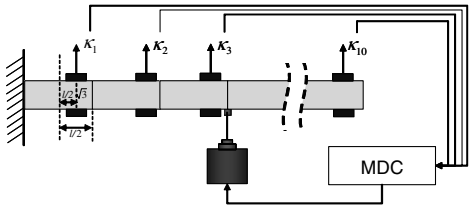

b) Strain output feedback

Fig. 1 Simulation scheme.

The results of case 1 are not available because of the divergence in the updated parameters. In spite of the same measurement errors in the displacement and strain mode shapes, the thickness of each beam element can be updated more accurately when the strain mode shapes are used. The reason for this phenomenon is that the condition number when we use the strain mode shapes is considerably less than when we use the displacement mode shapes. Note, in particular, that the case of the strain mode shapes with the closed-loop modes is more effective than any of the other cases.

V. Conclusions

Modal data such as natural frequencies and mode shapes are widely used in model updating. Strain mode shapes, in particular, have great potential for model updating applications because they are sensitive to local changes in structure. Although strain mode shapes have advantages over displacement mode shapes, problems still arise as a result of insufficient modal data. To prevent this problem, we use a mode decoupling controller that can increase the amount of modal data. We, consequently, propose a novel method of combining the strain mode shapes and the closed-loop scheme for effective model updating. The reason for combining them is to decrease the condition number of the combined modal sensitivity, thereby enhancing the performance of the model updating. Although the proposed method has great advantages, it also has two main limitations. To measure the strain mode shapes, we need to use more strain sensors than accelerometers for the displacement mode shapes. For more complex structures, this requirement is problematic. Secondly, due to limitations of the mode decoupling controller, if we change the strain mode shape too much in the closed loop, the system can become unstable. Overcoming these limitations is a goal of future research.

Acknowledgments

This work was supported by the Korea Science and Engineering Foundation (KOSEF) through a grant from the National Research Laboratory Program, which is funded by the Ministry of Science and Technology (2000-N-NL-01-C-148, M10500000112-05J0000-11210), and the Brain Korea 21 project of the Republic of Korea.

References

[1] Mottershead, J. E., and Friswell, M. I., "Model Updating in Structural Dynamics: A Survey," *Journal of Sound and Vibration*, Vol. 167, No. 2, 1993, pp. 347–375.

[2] Friswell, M. I., *Finite Element Model Updating in Structural Dynamics*, 1st ed., Kluwer Academic, London, 1996, Chap. 8.

[3] Jung, H., and Park, Y., "Model Updating Using the Closed-Loop Natural Frequency," *Journal of Guidance, Control, and Dynamics*, Vol. 28, No. 1, 2005, pp. 20–29.

[4] Jung, H., Park, Y., and Park, K. C., "Mode Decoupling Controller for Feedback Model Updating," *Proceedings of International Mechanical Engineering Congress and Exposition '04*, IMECE2004-59697, ASME, Anaheim, CA, 13–19 Sept. 2004.

[5] Pandey, A. K., Biswass, M., and Samman, M. M., "Damage Detection from Changes in Curvature Mode Shapes," *Journal of Sound and Vibration*, Vol. 145, No. 2, 1991, pp. 321–332.

[6] Yam, L. H., Leung, T. P., Li, D. B., and Xue, K. Z., "Theoretical and Experimental Study of Modal Strain Analysis," *Journal of Sound and Vibration*, Vol. 191, No. 2, 1996, pp. 251–260.

[7] Reich, G. W., and Park, K. C., "A Theory for Strain-Based Structural System Identification," *Journal of Applied Mechanics*, Vol. 68, No. 4, 2001, pp. 521–527.

[8] Adhikari, S., and Friswell, M. I., "Eigenderivative Analysis of Asymmetric Non-Conservative Systems," *International Journal for Numerical Methods in Engineering*, Vol. 51, No. 6, 2001, pp. 709–733.
[9] Gawronski, W. K., *Advanced Structural Dynamics and Active Control of Structures*, Springer–Verlag, New York, 2004, Chap. 8.
[10] Barlow, J., "Optimal Stress Locations in Finite Element Models," *International Journal for Numerical Methods in Engineering*, Vol. 10, No. 2, 1976, pp. 243–251.